Journal of Power Sources 244 (2013) 565–569

Contents lists available at SciVerse ScienceDirect

Journal of Power Sources

journal homepage: www.elsevier.com/locate/jpowsour

Short communication

Electrochemical properties of chemically modified phosphoolivines as cathode materials for Li-ion batteries

Andrzej Kulka, Dominika Baster, Michał Dudek, Michał Kiełbasa, Anna Milewska, Wojciech Zając, Konrad Świerczek, Janina Molenda*

AGH University of Science and Technology, Faculty of Energy and Fuels, Department of Hydrogen Energy, al. A. Mickiewicza 30, 30-059 Krakow, Poland

HIGHLIGHTS

- Chemical modification of $LiFePO_4$ possible only in case of Fe-site substitution.
- Modified $LiFePO_4$ stable against $LiPF_6$-EC–DEC electrolyte.
- Enhanced conductivity of modified $LiFePO_4$ not linked to electrochemical performance.
- The best electrochemical performance obtained for unmodified nano-sized $LiFePO_4$.

ARTICLE INFO

Article history:
Received 22 October 2012
Received in revised form
24 January 2013
Accepted 28 January 2013
Available online 5 February 2013

Keywords:
$LiFePO_4$
Doping
Cathode materials
Electrochemical properties
Chemical stability

ABSTRACT

Li-site, Fe-site and P-site substituted $LiFePO_4$ phosphoolivines were synthesized and examined in terms of crystal structure, electrical conductivity, charge–discharge performance in $Li/Li^+/LiFePO_4$-type cells, as well as chemical stability against the $LiPF_6$-EC–DEC electrolyte. Despite possible improvement of electrical conductivity of the substituted phosphoolivines, it seems that the optimization of morphology and reduction of grain size is the most efficient way of improvement of electrochemical performance of $LiFePO_4$, while chemical stability of the substituted materials remains high.

1. Introduction

Nowadays, $LiFePO_4$ is considered as one of the most promising cathode materials for Li-ion technology, including application in hybrid and electric vehicles or renewable energy systems [1–3]. Due to its low electrical conductivity, preparation of effectively working $LiFePO_4$-based cathode is complex and requires optimization of both, cathode material itself, as well as conductive additives [4–7]. Since lithium diffusion coefficient is low, of the order of 10^{-16}–10^{-11} cm^2 s^{-1}, which stems from 1-dimensional-type diffusion, transition to the nano-scale is an effective way of improvement of electrochemical properties of $LiFePO_4$. As hopping of Li^+ is preferential along *b*-axis [8,9], morphology of nano-grains with well-developed (010) surfaces is beneficial. Additionally to grain morphology engineering, also doping of phosphoolivine in Li sublattice was proposed as a way of improvement of properties [10], but the results were questioned, and it was found that increase of the electrical conductivity was due to a formation of phosphides and/or carbo-phosphides on surface of phosphoolivine grains [11,12]. There is an ongoing discussion in the literature if substitution in lithium sublattice in $LiFePO_4$ can actually take place [10,13–26]. On the other hand, substitution of Fe by other 3*d* metals (e.g. Mn, Co or Ni) was proven to be possible in the whole concentration range [27–29], but it does not bring pronounced enhancement of transport properties of the materials, but rather their deterioration. However, such substitution provides new, higher potential plateaus, related to M^{2+}/M^{3+} (M: Mn, Co, Ni) redox couples [30,31]. One can also imagine substitution of P^{5+} in tetrahedral sites in $LiFePO_4$ by other elements, but until now data about such modification are very limited and do not unambiguously support or exclude such possibility [32,33]. In this work we present results of electrochemical studies, along with data on chemical

* Corresponding author.
E-mail address: molenda@agh.edu.pl (J. Molenda).

0378-7753/$ – see front matter © 2013 Elsevier B.V. All rights reserved.
http://dx.doi.org/10.1016/j.jpowsour.2013.01.156

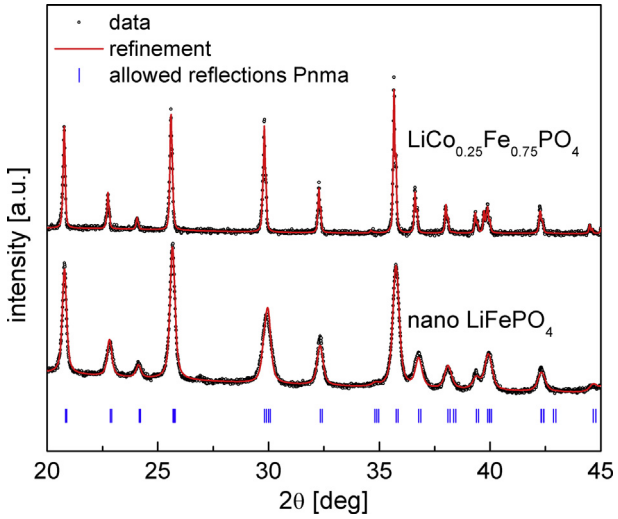

Fig. 1. XRD patterns for nano-$LiFePO_4$ (lower part) and high-temperature synthesized $LiFe_{0.75}Co_{0.25}PO_4$ (upper part).

stability of $LiFePO_4$-related materials against liquid electrolyte concerning nano-sized $LiFePO_4$, as well as materials with assumed Li-site, Fe-site or P-site substitution.

2. Experimental

Nano-sized $LiFePO_4$ powder was obtained by a low temperature method developed by Delacourt et al. [34]. The method is based on precipitation from 1:1 vol. water–ethylene glycol solution. Boiling solutions of 0.1 mol dm^{-3} $FeSO_4$ (Fluka, 99.5%), 0.1 mol dm^{-3} H_3PO_4 (Chempur, 85%) and 0.3 mol dm^{-3} LiOH – (Chempur, 99%) were mixed and the green-grayish precipitate was aged overnight under reflux condenser. The obtained material was filtered, flushed with distilled water and isopropanol, and dried in vacuum at 50 °C. Synthesized powder was annealed at 300 °C in 5 vol.% H_2 in Ar flow. $LiFe_{1-x}M_xPO_4$ (M = Mn, Co and Ni; x = 0, 0.25, 0.5, 0.75 and 1) materials were synthesized using high-temperature method. Stoichiometric amounts of Li_2CO_3 (POCH, 99%), $NH_4H_2PO_4$ (POCH, 98%), $FeC_2O_4{\cdot}2H_2O$ (Aldrich, 99%), $MnCO_3$ (Chempur, 99%), $Ni(OH)_2$ (Aldrich, 95%) and $CoCO_3$ (Acros Organics, 90%) were thoroughly milled, pressed into pellets and heated at 750 °C for 12 h in Ar atmosphere with two intermediate steps at 100 and 350 °C. For this work we concentrated on studying only samples with $x = 0.25$ mol mol^{-1}, due to their enhanced electrical conductivity, as comparing to the pristine $LiFePO_4$. Li-site substituted series with assumed chemical compositions: $Li_{0.97}Al_{0.01}FePO_4$, $Li_{0.96}Zr_{0.01}FePO_4$ and $Li_{0.94}W_{0.01}FePO_4$ were synthesized using high-temperature method, details of the procedure were described in Ref. [26]. The same method was used for preparation P-site doped phosphoolivines with assumed composition $LiFeP_{1-6/5y}W_yO_4$ and $LiFeP_{1-6/5y}Mo_yO_4$. The value of y was chosen to be 0.01, 0.05 and 0.1 mol mol^{-1}. X-ray diffraction (XRD) experiments were performed on a Panalytical X'PERT pro diffractometer with CuK_α radiation. The phase composition of the prepared samples was confirmed using data from PDF2 database. Unit cell parameters of the materials were determined by Rietveld refinement method with GSAS/EXPGUI set of software [35,36]. SEM measurements were conducted on FEI Nova NanoSEM 200 apparatus working with Low Vacuum Detector (LVD). The grain size was estimated on the basis of SEM measurements and XRD peaks broadening using Scherrer's formula. In the case of materials obtained by solid-state synthesis method (Li-site, Fe-site and P-site substituted samples), diffraction peak broadening was comparable with the instrument broadening, so application of this method was not possible. Electrical conductivity was measured by means of 4-probe DC method on cuboid sinters. Studies were performed under constant flow of Ar gas. Electrochemical studies were carried out in $Li/Li^+/LiFePO_4$ cells assembled using CR2032-type containers. 1 M solution of $LiPF_6$ in ethylene carbonate/diethyl carbonate (EC/DEC) was used as the electrolyte. For the positive electrode, the active material was mixed with polytetrafluoroethylene (PVDF) as a binder and graphite/carbon black (for electronic conduction enhancement) in a 70:5:15:10 mass ratio. *N*-Methyl-2-pyrrolidone (NMP) was added to get proper viscosity of the obtained paste. The slurry was then coated on an Al foil and dried at 70 °C in a vacuum dryer. Electrochemical cells were assembled in a glove box (UNILAB, M. Braun) under argon atmosphere with controlled oxygen and water vapor pressure. Electrochemical measurements were performed on KEST 32k multichannel galvanostat. The cut-off voltages were set as 2.5 V on discharge and 4.3 V on charge. The exceptions were Fe-site doped materials, for which 5.1 V cut-off was set, in order to observe high-voltage redox potentials of $Mn^{2+/3+}$, $Co^{2+/3+}$ and $Ni^{2+/3+}$. Due to instability of the electrolyte, higher voltages could not be recorded in electrochemical studies. Differential Scanning Calorimetry (DSC) experiments were performed in Mettler-Toledo 821e calorimeter equipped with an intracooler Haake in 40 μl aluminum crucibles closed by lid with a hole (Φ = 0.2 mm) under constant flow of argon (80 ml min^{-1}) within temperature range 25–450 °C and the heating rate of 10 °C min^{-1}. A small amount of the cathode material sample was carefully pressed into bottom of the crucible and wetted with one droplet of $LiPF_6$-EC–DEC electrolyte.

3. Results and discussion

In order to evaluate the influence of chemical substitution on electrochemical properties of phosphoolivine, several materials with assumed Li-site, Fe-site or P-site substitution were studied and the obtained results were compared with the optimized, nano-sized $LiFePO_4$.

Table 1
Unit cell parameters of the studied phosphoolivines. Space group *Pnma*. Numbers in brackets denotes error from Rietveld refinement.

	a [Å]	b [Å]	c [Å]	V [Å^3]	R_{wp}	R_p	Reference
nano-$LiFePO_4$	10.3304(7)	5.9791(4)	4.7093(4)	290.95(1)	5.45	4.32	This work
$LiFe_{0.75}Mn_{0.25}PO_4$	10.3603(1)	6.0296(1)	4.7045(1)	293.88(1)	6.63	5.24	This work
$LiFe_{0.75}Co_{0.25}PO_4$	10.2973(1)	5.9872(1)	4.6933(1)	289.35(1)	1.83	1.43	This work
$LiFe_{0.75}Ni_{0.25}PO_4$	10.2558(1)	5.9777(1)	4.6897(1)	287.51(1)	9.60	7.62	This work
$Li_{0.97}Al_{0.01}FePO_4$	10.3275(2)	6.0072(1)	4.6932(1)	291.16(3)	4.22	3.36	[37]
$Li_{0.96}Zr_{0.01}FePO_4$	10.3284(8)	6.0078(4)	4.6938(5)	291.25(5)	5.22	4.11	[26]
$Li_{0.94}W_{0.01}FePO_4$[a]	10.3317(1)	6.0080(7)	4.6933(2)	291.32(7)	4.43	3.50	[26]
$LiFeP_{0.88}Mo_{0.10}O_4$	10.3293(3)	6.0088(2)	4.6936(2)	291.32(3)	7.99	6.32	This work

[a] Traces of secondary FeWO4 phase were detected.

3.1. X-ray diffraction and morphology

In Fig. 1 exemplary XRD patterns for $LiFe_{0.75}Co_{0.25}PO_4$ prepared by a high-temperature method and nano-$LiFePO_4$ prepared a low-temperature method are shown. Table 1 gathers refined unit cell parameters of synthesized nano-$LiFePO_4$, as well as data for other materials used in this study: $LiFe_{0.75}Mn_{0.25}PO_4$, $LiFe_{0.75}Co_{0.25}PO_4$, $LiFe_{0.75}Ni_{0.25}PO_4$, $Li_{0.97}Al_{0.01}FePO_4$, $Li_{0.96}Zr_{0.01}FePO_4$, $Li_{0.94}W_{0.01}FePO_4$ and $LiFeP_{0.88}Mo_{0.10}O_4$. One can notice much broader diffraction peaks in the case of nano-sized $LiFePO_4$, in comparison with high-temperature synthesized $LiFe_{0.75}Co_{0.25}PO_4$ with micrometer-size grains. All other high-temperature samples exhibited similar, relatively narrow peaks. The estimated average crystallite size, determined on a basis of Scherrer's formula was 50 nm for nano-sized $LiFePO_4$. Differences in crystallite size between these materials were confirmed by SEM measurements. In Fig. 2 SEM micrographs are presented: nano-sized $LiFePO_4$ sample consists of platelet grains (crystallites), which average size was estimated to be equal 50 × 500 × 500 nm. These platelets are congregated into bigger agglomerates. In the case of $LiFe_{0.75}Co_{0.25}PO_4$ sample, the average grain size is equal to 3 μm, as given by statistical analysis of SEM micrograph.

3.2. Summary of structural behavior of Li, Fe and P-site doped $LiFePO_4$

Analysis of X-ray diffraction patterns of $LiFe_{1-x}M_xPO_4$ (M = Mn, Co and Ni) compounds in whole substitution range ($0 \le x \le 1$) points to a formation of single-phase solid solutions in the whole considered range *x*. This result was supported by a linear variation of unit cell parameters, for samples with particular M, recorded for all *x* values. This is an expected behavior, due to Vegard's rule for formation of solid state solution. For examination of electrochemical properties, we selected samples with $x = 0.25$, which exhibit enhanced electrical conductivity. In the previous work [26] we showed limited solid solution formation in the case of Li-site doping of phosphoolivine, and based on these results, only samples with Al, Zr and W substitution equal 0.01, which are not contaminated by substantial amounts of additional phases, were selected for the presented studies. In the case of samples with assumed P-site substitution, XRD data for $LiFeP_{1-6/5y}W_yO_4$ shows formation of $FeWO_4$, which amount is proportional to the substitution level *y*, suggesting that it is impossible to introduce W^{6+} into tetrahedral P-sites. Interestingly, in case of Mo, no additional peaks were identified on X-ray patterns, even in the case of relatively high level of substitution in the sample with composition $LiFeP_{0.88}Mo_{0.10}O_4$. However, unit cell parameters did not change considerably, suggesting that the actual substitution does not take place. We assume that Mo-rich phase, present in the materials is amorphous. As shown by J. Hong et al. [37], also vanadium, despite its similarity to phosphorus, preferentially occupies iron sites in the phosphoolivine lattice, which supports lack of possibility of modification of the phosphorus sublattice.

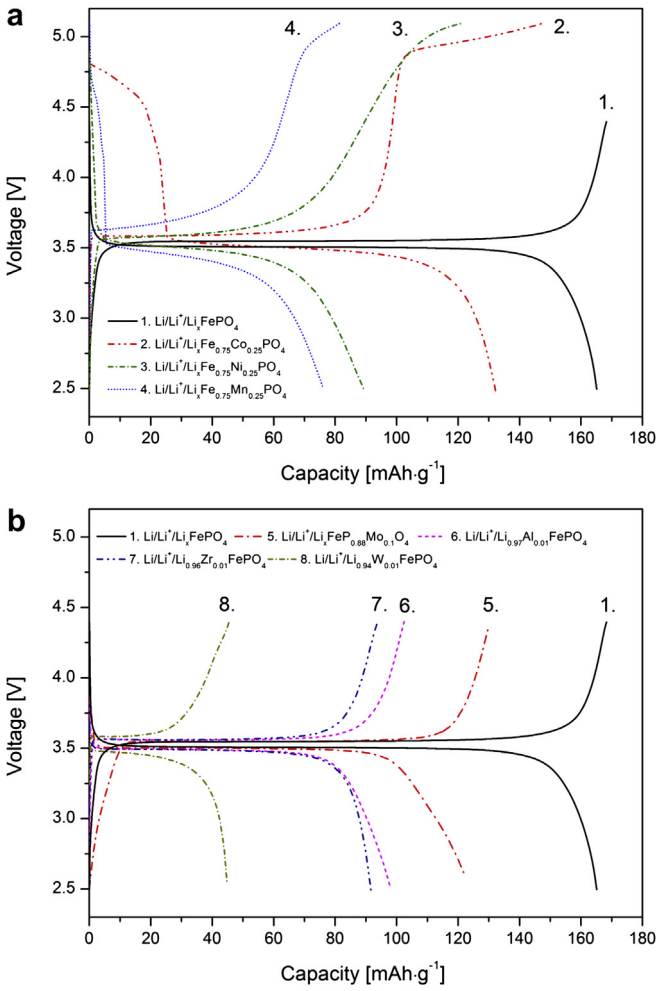

Fig. 3. Charge/discharge curves recorded with 0.1 C rate for nano-$LiFePO_4$ compared with a) Fe-site substituted $LiFePO_4$ and b) Li-site and P-site substituted $LiFePO_4$.

3.3. Electrochemical properties

Voltage profiles during charge and discharge processes (second cycle) of $Li/Li^+/LiFePO_4$-type cells are presented in Fig. 3a and b. All

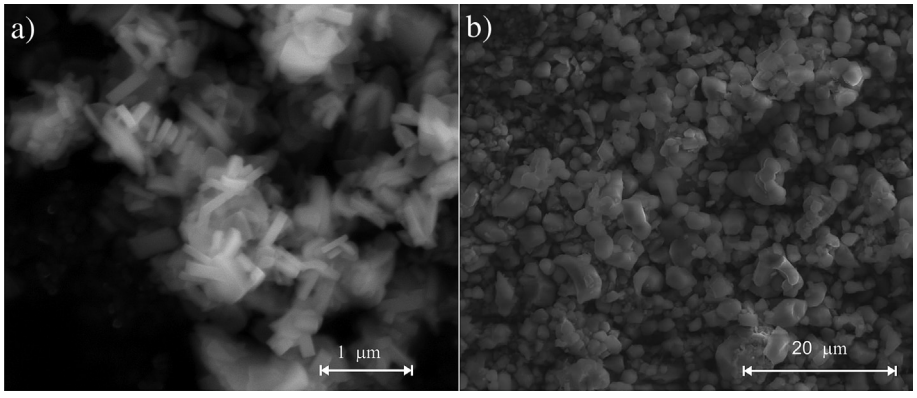

Fig. 2. SEM micrographs of a) nano-$LiFePO_4$ and b) high-temperature synthesized $LiFe_{0.75}Co_{0.25}PO_4$.

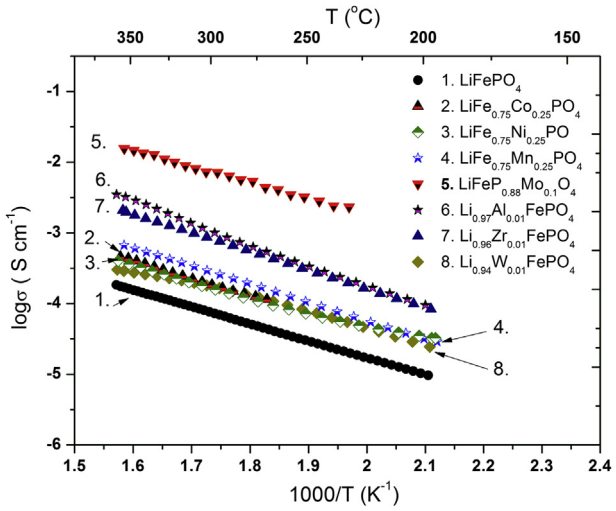

Fig. 4. Electrical conductivity dependence on temperature for chemically modified phosphoolivines.

measured curves present plateau at around 3.5 V, which is related to redox reaction of Fe^{2+}/Fe^{3+} in phosphoolivine. For the Fe-site substituted samples, due to 0.25 mol mol^{-1} substitution, during charge a second plateau was observed at higher voltages, but on discharge, the only sample with substantial capacity at higher voltages was $LiFe_{0.75}Co_{0.25}PO_4$. The ratio of $Co^{2+/3+}$-related capacity in relation to $Fe^{2+/3+}$ capacity is approximately equal the theoretical one expected owning to chemical composition (1:4). Lack of $Mn^{2+/3+}$ and $Ni^{2+/3+}$-related discharge capacities can be seen. This originates from a large polarization of the cells, which also suggests high internal resistance in the studied range of potentials. Another unresolved issue, which has to be addressed before utilization of the full capacity of Fe-site substituted materials is electrochemical stability of the electrolyte at high voltages. Both these factors strongly limit the application of Fe-site doped materials.

3.4. Electrical conductivity and rate performance

Considering the second group of studied compositions, small Li-site substitution should not contract Fe-connected electrochemical capacity of the cell, and may bring improvement of the electrical conductivity of the cathode material [38], which is actually observed in the presented studies (Fig. 4). However, due to blocking of 1-dimensional Li diffusion paths by substituted cations, worsening of the electrochemical properties can be expected. This indeed is the case, which can be seen in Fig. 3b. Among chemically modified materials, the best performance was observed for the P-site molybdenum substituted sample. The resulting discharge capacity was close to 120 mAh g^{-1}. This may be related to the above-mentioned glass-like Mo-containing phase. The measured electrical conductivity of this material was determined to be two orders of magnitude higher than pristine $LiFePO_4$ (Fig. 4). This, in turn, may improve transport properties of the cathode, as glassy layer was shown to be highly beneficial in terms of electrochemical performance [39]. Electrical conductivity at room temperature along with activation energy values for the studied materials are

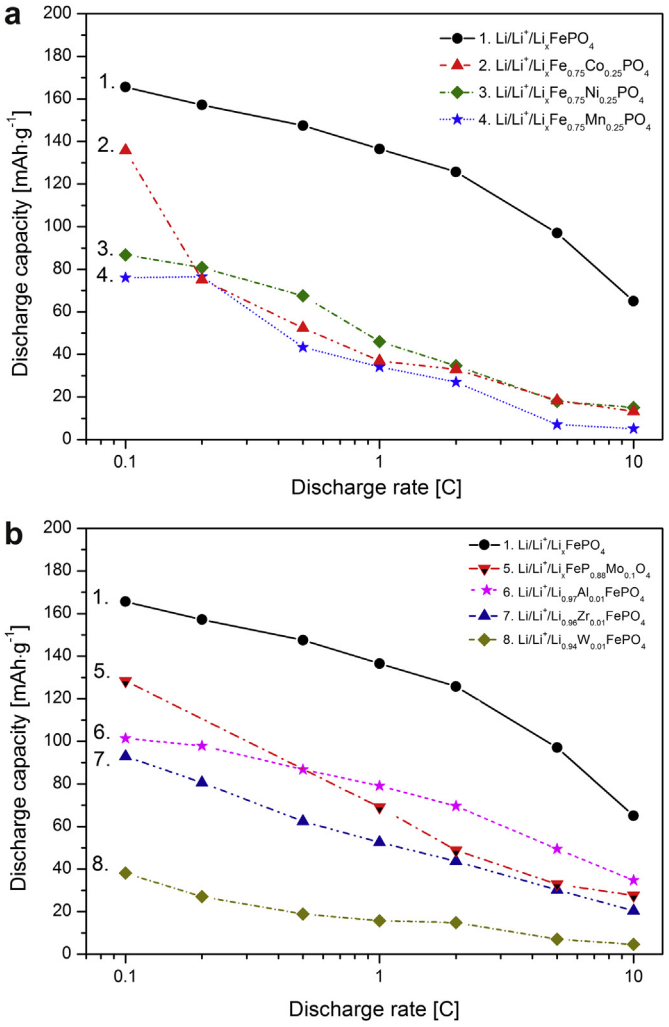

Fig. 5. Dependence of reversible capacity of Li/Li^+/phosphoolivine cells as a function of discharge rate for nano-$LiFePO_4$ compared with a) Fe-site substituted $LiFePO_4$ and b) Li-site and P-site substituted $LiFePO_4$.

gathered in Table 2. Nevertheless, the highest, close to the theoretical, capacity was measured in the case of nano-sized, undoped $LiFePO_4$. This points to the dominating effect of grain morphology and a preparation procedure on the electrochemical properties of $LiFePO_4$-based materials. Apart from the highest capacity, nano-sized material also shows the best performance for high currents: for 1 C discharge rate, the capacity was about 135 mAh g^{-1}, while for 10 C it was still 65 mAh g^{-1} (Fig. 5a and b). No other material performed close to these values, what is especially visible at higher currents.

3.5. Chemical stability vs. lithium electrolyte

Fig. 6a and b gather results of DSC measurements of chemical stability of considered cathode materials with $LiPF_6$-based electrolyte. Two endothermic peaks (near 150 and 250 °C) in Fig. 6a and

Table 2
Obtained values of activation energy E_a (eV) and extrapolated values of electrical conductivity σ (S cm^{-1}) at room temperature.

	$LiFePO_4$	$LiFe_{0.75}Co_{0.25}PO_4$	$LiFe_{0.75}Ni_{0.25}PO_4$	$LiFe_{0.75}Mn_{0.25}PO_4$	$LiFeP_{0.88}Mo_{0.1}O_4$	$Li_{0.97}Al_{0.01}FePO_4$	$Li_{0.96}Zr_{0.01}FePO_4$	$Li_{0.94}W_{0.01}FePO_4$
E_a	0.48	0.49	0.46	0.51	0.44	0.60	0.53	0.46
log σ	−8.03	−7.76	−7.50	−7.74	−5.77	−7.83	−7.38	−7.51

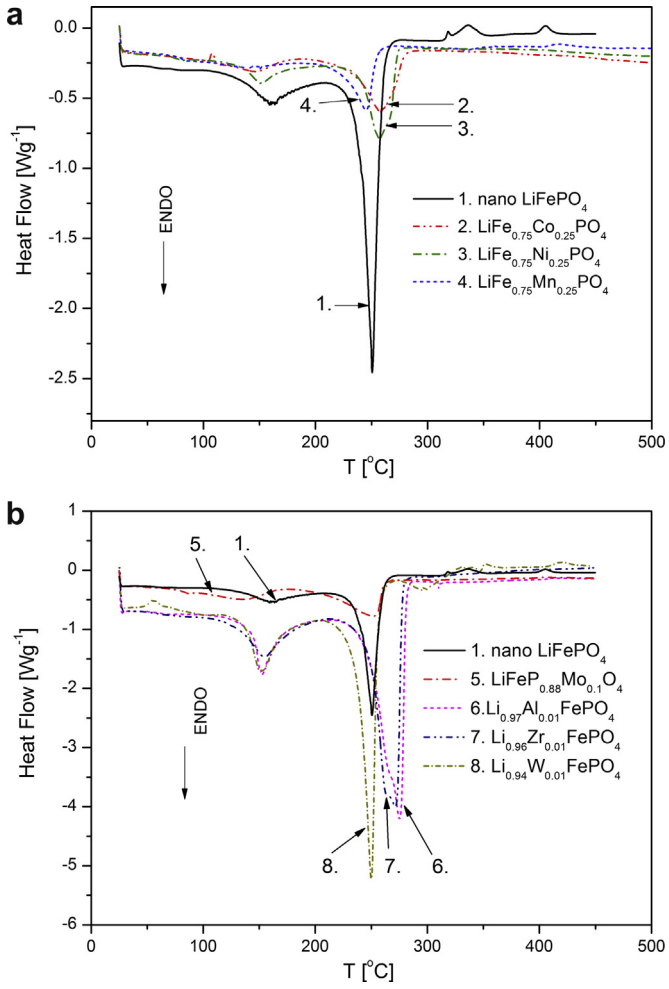

Fig. 6. Recorded DSC curves for nano-$LiFePO_4$ compared with a) Fe-site substituted $LiFePO_4$ and b) Li-site and P-site substituted $LiFePO_4$ being in contact with $LiPF_6$-EC–DEC electrolyte.

b can be attributed to the evaporation of organic solvents of Li^+ electrolyte, diethyl carbonate (DEC) and ethylene carbonate (EC) with boiling temperatures about 130 °C and 260 °C respectively. Lack of visible exothermic peaks shows stability of the materials vs. considered lithium electrolyte. This is in the contrary to situation, in which cathode material reacts with an electrolyte, which was observed for instance in the case of $LiNi_{1-y-z}Co_yMn_zO_2$ layered oxides, where clearly visible exothermic peaks on DSC curves were recorded at about 325 °C [40,41] For all presented curves no such effect is visible (apart from nano-$LiFePO_4$, where small signals between 300 and 450 °C was observed), which suggests that chemical modification of phosphoolivine has no significant influence on the stability of the considered materials in relation to the $LiPF_6$-EC–DEC electrolyte.

4. Conclusions

Chemical modification of $LiFePO_4$ may be effectively realized only in the case of Fe-site substitution. For samples with assumed Li-site and P-site modification the formation of solid solution is either impossible or limited to very narrow range of doping level. Interestingly, for $LiFeP_{0.88}Mo_{0.10}O_4$ material, lack of visible additional peaks on XRD data suggest formation of glass-like, Mo-containing phases. Macroscopic, electrical conductivity of modified samples may be enhanced, and for the mentioned $LiFeP_{0.88}Mo_{0.10}O_4$ composition such enhancement is about two orders of magnitude. Nevertheless, electrochemical performance of this material is worse, comparing to nano-$LiFePO_4$. Optimization of morphology and reduction of grain size seems to be the most efficient way of improvement of performance of $LiFePO_4$. At the same time chemical modification does not affect stability of the substituted materials against $LiPF_6$-EC–DEC electrolyte, and remains high.

Acknowledgments

This work was financially supported by EU under the grant No. UDA-POIG 01.01.02-00-108/09-05 and European Institute of Innovation and Technology, under KIC InnoEnergy NewMat project.

References

[1] G.A. Nazri, G. Pistoia, Lithium Batteries Science and Technology, Springer, 2003.
[2] J. Molenda, Funct. Mater. Lett. 4 (2011) 107–112.
[3] K. Ozawa, Lithium Ion Rechargeable Batteries, Wiley-Vch, 2009.
[4] O. Toprakci, H.A.K. Toprakci, Liwen Ji, Xiangwu Zhang, KONA Powder Part. J. 28 (2010) 50–73.
[5] K. Zaghib, A. Mauger, C.M. Julien, J. Solid State Electrochem. 16 (2012) 835–845.
[6] J. Wang, X. Sun, Energy Environ. Sci. 5 (2012) 5163–5185.
[7] L.-X. Yuan, Z.-H. Wang, W.-X. Zhang, X.-L. Hu, J.-T. Chen, Y.-H. Huang, J.B. Goodenough, Energy Environ. Sci. 4 (2011) 269–284.
[8] D. Morgan, A. Van der Ven, G. Ceder, Electrochem. Solid State Lett. 7 (2004) A30–A32.
[9] R. Amin, P. Balaya, J. Maier, Electrochem. Solid State Lett. 10 (2007) A13–A16.
[10] S.Y. Chung, J.T. Bloking, Y.M. Chiang, Nat. Mater. 1 (2002) 123–128.
[11] P.S. Herle, B. Ellis, N. Coombs, L.F. Nazar, Nat. Mater. 3 (2004) 147–152.
[12] W. Ojczyk, J. Marzec, K. Świerczek, W. Zając, M. Molenda, R. Dziembaj, J. Molenda, J. Power Sources 173 (2007) 700–706.
[13] M.S. Islam, D.J. Driscoll, C.A.J. Fisher, P.R. Slater, Chem. Mater. 17 (2005) 5085–5092.
[14] S.Y. Chung, Y.-M. Chiang, Electrochem. Solid State Lett. 12 (2003) A278–A281.
[15] M. Wagemaker, B.L. Ellis, D. Lutzenkirchen-Hecht, F.M. Mulder, L.F. Nazar, Chem. Mater. 20 (2008) 6313–6315.
[16] R. Yang, X. Song, M. Zhao, F. Wang, J. Alloys Compd. 22 (2009) 365.
[17] D. Li, Y. Huang, D. Jia, Z. Guo, S.-J. Bao, J. Solid State Electrochem. 14 (2010) 889–895.
[18] M.R. Roberts, G. Vitins, J.R. Owen, J. Power Sources 179 (2008) 754–762.
[19] Z. Peixin, W. Yanxuan, L. Jianhong, X. Qiming, R. Xiangzhong, Z. Qianling, L. Zhongkuan, Rare Met. Mat. Eng. 36 (2007) 954.
[20] D. Zhuang, X. Zhao, J. Xie, J. Tu, T. Zhu, G. Cao, Acta Phys Chim. Sin. 22 (2006) 840–844.
[21] X.Y. Wen, M.P. Zheng, Z.F. Tong, J. Inorg. Mater. 21 (2006) 115.
[22] O. Chu-Ying, W. De-Yu, S. Si-Qi, W. Zhao-Xiang, L. Hong, H. Xue-Jie, C. Li-Quan, Chin. Phys. Lett. 23 (2006) 61–64.
[23] C. Delacourt, C. Wurm, L. Laffont, J.-B. Leriche, C. Masquelier, Solid State Ionics 3-4 (2006) 333–341.
[24] C.Y. Ouyang, S.Q. Shi, Z.X. Wang, H. Li, X.J. Huang, L.Q. Chen, J. Phys. Condens. Matter. 16 (2004) 2265–2272.
[25] S. Shi, L. Liu, C. Ouyang, D.-S. Wang, Z. Wang, L. Chen, X. Huang, Phys. Rev. B 68 (2003) 195108.
[26] A. Kulka, A. Milewska, W. Zając, K. Świerczek, E. Hanc, J. Molenda, Solid State Ionics 225 (2012) 575–579.
[27] J. Molenda, W. Ojczyk, J. Marzec, J. Power Sources 174 (2007) 689–694.
[28] Y. Gea, X. Yanc, J. Liua, X. Zhanga, J. Wanga, X. Hea, R. Wanga, H. Xi, Electrochim. Acta 55 (2010) 5886–5890.
[29] A. Perea, M.T. Sougrati, C.M. Ionica-Bousquet, B. Fraisse, C. Tessier, L. Aldona, J.-C. Jumasa, RSC Adv. 2 (2012) 2080–2086.
[30] T. Muraliganth, A. Manthiram, J. Phys. Chem. C 114 (2010) 15530–15540.
[31] J. Wolfenstine, J. Allen, J. Power Sources 142 (2005) 389–390.
[32] Z. Wang, S. Sun, D. Xia, W. Chu, S. Zhang, Z. Wu, J. Phys. Chem. C 112 (2008) 17450–17455.
[33] Y. Wang, Z.-S. Feng, J.-J. Chen, C. Zhang, X. Jin, J. Hu, Solid State Commun. 152 (2012) 1577–1580.
[34] C. Delacourt, P. Poizot, S. Levasseur, C. Masquelier, Electrochem. Solid State Lett. 9 (2006) A352–355.
[35] A.C. Larson, R.B. Von Dreele, Los Alamos Natl. Lab. Rep. – LAUR 86–-748, (2004).
[36] B.H. Toby, J. Appl. Crystallogr. 34 (2001) 210–213.
[37] J. Hong, X.-L. Wang, Q. Wang, F. Omenya, N.A. Chernova, M.S. Whittingham, J. Graetz, J. Phys. Chem. C 116 (2012) 20787–20793.
[38] M. Kimura, K. Świerczek, J. Marzec, J. Molenda, Funct. Mater. Lett. 4 (2011) 123–127.
[39] B. Kang, G. Ceder, Nature 458 (2009) 190–193.
[40] A. Milewska, M. Molenda, J. Molenda, Solid State Ionics 192 (2011) 313–320.
[41] M. Molenda, R. Dziembaj, Z. Piwowarska, M. Drozdek, Solid State Ionics 179 (2008) 88–92.